

High-dimensional GARCH process segmentation with an application to Value-at-Risk

Haeran Cho

School of Mathematics, University of Bristol

and

Karolos K. Korkas*

Citigroup

June 21, 2022

Abstract

An assumption in modelling financial risk is that the underlying asset returns are stationary. However, there is now strong evidence that multivariate financial time series entail changes not only in their within-series dependence structure, but also in the correlations among them. For this reason, we propose a method for consistent detection of multiple change-points in (possibly high) N -dimensional GARCH panel data set, where both individual GARCH processes and their correlations are allowed to change. We prove its consistency in multiple change-point estimation, and demonstrate its good performance through an extensive simulation study and an application to the Value-at-Risk problem on a real dataset. Our methodology is implemented in the R package `segMGarch`, available from CRAN.

Key words and phrases: multiple change-point detection, multivariate GARCH, stress period selection, Double CUSUM Binary Segmentation, high dimensionality, nonstationarity

*DISCLAIMER: The views and opinions rendered in this article reflect the authors personal views about the subject and do not necessarily represent the views of Citigroup Inc. or any part thereof.

1 Introduction

The increased financial uncertainty during the recent global economic crisis has confirmed the close volatility linkage between asset markets. For example, there is now strong evidence that the economy and oil prices ([Hamilton, 2003](#)), foreign exchange rates ([Baillie, 1991](#)), equity markets ([Baele, 2003](#)) and crude oil and agricultural commodities ([Du et al., 2011](#)) are related. These co-movements are naturally expected since the rate of information influences the volatility in asset returns and therefore, the information flow from one asset market can be incorporated into another related market ([Ross, 1989](#)). Therefore, good understanding of the correlations among multiple markets is crucial for policy makers, financial institutions and investors.

The joint modelling of financial returns as Multivariate GARCH processes has attracted considerable attention in the literature, and the proposed models include the vectorised multivariate GARCH model ([Bollerslev et al., 1988](#)), Baba-Engle-Kraft-Kroner (BEKK) model ([Engle and Kroner, 1995](#)), constant conditional correlation (CCC) model ([Bollerslev, 1990](#)), dynamic conditional correlation (DCC) model ([Engle, 2002](#)), generalised orthogonal GARCH model ([Van der Weide, 2002](#)), full-factor multivariate GARCH model ([Vrontos et al., 2003](#)) and conditionally uncorrelated components-based multivariate volatility processes ([Fan et al., 2008](#)); for a survey of multivariate GARCH modelling and inference, see [Bauwens et al. \(2006\)](#).

The assumption that the underlying dynamics remain unchanged is restrictive considering that the fundamentals driving an economy, the asset markets in particular, exhibit sudden changes or regimes switches. Empirical evidence of change-points (a.k.a. structural breaks or breakpoints) in various macroeconomic and financial time series are well documented, see [Hansen \(2001\)](#), [Stock and Watson \(2002\)](#) and [Barigozzi et al. \(2018\)](#) among many others. [Pesaran and Timmermann \(2007\)](#) examined eight major currency pairs and established that stationary volatility modelling induces an upward bias in the mean square forecast error when change-points exist in the exchange rate volatility.

[Cappiello et al. \(2006\)](#) documented a change-point in the correlations between international equity and bond returns after the introduction of the Euro currency, supporting the need for

a method that accounts for change-points in both the conditional volatility and correlation. [Ewing and Malik \(2013\)](#) found a significant stronger transmission of volatility (spillover) between oil and gold prices when change-points in their variance were accounted for. [Diebold and Inoue \(2001\)](#) and [Mikosch and Stărică \(2004\)](#) noted that stochastic regime switching may be confused with long-range dependence. In this paper, we observe the importance of accounting for the structural breaks in the volatilities and correlations of a multi-asset portfolio. In particular, we show that the stressed Value-at-Risk, a popular measure of market risk widely adopted by financial institutions, under-estimates the exposure of a portfolio when a pre-selected period of a fixed length is used as the stress period, rather than the most volatile period identified by the structural breaks.

Investigations into the tests for a *single* structural break in univariate conditional heteroscedastic models have been made in [Kokoszka and Leipus \(2000\)](#), [Kokoszka and Teyssière \(2002\)](#), [Lee et al. \(2003\)](#), [Berkes et al. \(2004\)](#) and [De Pooter and Van Dijk \(2004\)](#). For multiple change-point detection, [Fryzlewicz and Subba Rao \(2014\)](#) proposed a two-stage procedure termed BASTA (binary segmentation for transformed ARCH) for detecting changes in the conditional variance of univariate series, while [Andreou and Ghysels \(2003\)](#) studied change-point detection in the co-movement of bivariate returns. More recent change-point methods for (conditional) covariance structure of multivariate data include [Dette et al. \(2018\)](#) and [Barassi et al. \(2018\)](#) on testing for a single change-point, or [Wang et al. \(2018\)](#) on estimating the multiple change-points.

In this paper, we propose a change-point methodology for multiple change-point detection in multivariate, possibly high-dimensional GARCH processes. It simultaneously segments high-dimensional GARCH processes by identifying ‘common’ change-points, each of which can be shared by a subset or all of the component time series as a change-point in their within-series and/or cross-sectional correlation structure. The methodology first transforms the N -dimensional time series into $N(N+1)/2$ -dimensional panel data consisting of empirical residual series and their cross-products, whereby change-points in the complex ((un)conditional variance and covariance) structure are made detectable as change-points in the simpler (mean) structure of the panel data at the price of the increased dimensionality. A number of method-

ologies have been investigated for change-point analysis in the means of high-dimensional panel data, such as [Horváth and Hušková \(2012\)](#), [Jirak \(2015\)](#), [Cho and Fryzlewicz \(2015\)](#) and [Wang and Samworth \(2018\)](#). Among many, we adopt the Double CUSUM Binary Segmentation procedure ([Cho, 2016](#)), which achieves consistency in estimating both the total number and locations of the multiple change-points while permitting within-series and cross-sectional correlations, for simultaneous segmentation of the panel data of transformed time series. Extending the mixing property originally derived for univariate, time-varying ARCH processes in [Fryzlewicz and Subba Rao \(2011\)](#) to that of time-varying bivariate GARCH processes, we establish the consistency of the combined methodology.

The rest of the paper is organised as follows. Section 2 introduces a time-varying multivariate GARCH model which provides a framework for the theoretical treatment of our methodology. Section 3 is devoted to the description of the proposed two-stage methodology and its theoretical properties. Its finite sample performance is investigated on sets of simulated data in Section 4 and a real financial dataset In Section 5. Section 6 concludes the paper, and the supplementary document provides all the proofs and additional simulation results. Our methodology is implemented in the R package `segMGarch`, available from CRAN.

Notation

For any set $\Pi \subset \{1, \dots, N\}$, we denote its cardinality by $|\Pi|$. For given observations $\{\mathbf{r}_t\}_t$, $\mathbf{r}_t \in \mathbb{R}^N$, we denote by \mathcal{F}_t the σ -algebra $\sigma\{\mathbf{r}_s, s \leq t\}$. Also, we use the notations $a \vee b = \max(a, b)$ and $a \wedge b = \min(a, b)$. Besides, $a \sim b$ indicates that a is of the order of b , and $a \gg b$ indicates that $a^{-1}b \rightarrow 0$. We denote a vector of zeros by $\mathbf{0}$ whose dimension should be clear from the context.

2 Time-varying multivariate GARCH model

We consider the following time-varying multivariate GARCH (tv-MGARCH) model denoted by $\mathbf{r}_t = (r_{1,t}, \dots, r_{N,t})^\top$, $t = 1, \dots, T$:

$$r_{i,t} = \sqrt{h_{i,t}} \varepsilon_{i,t} \quad \text{where} \quad (1)$$

$$h_{i,t} = \omega_i(t) + \sum_{j=1}^p \alpha_{i,j}(t) r_{i,t-j}^2 + \sum_{k=1}^q \beta_{i,k}(t) h_{i,t-k}. \quad (2)$$

The independent innovations $\boldsymbol{\varepsilon}_t = (\varepsilon_{1,t}, \dots, \varepsilon_{N,t})^\top$ satisfy $\mathbb{E}(\boldsymbol{\varepsilon}_t) = \mathbf{0}_N$ and $\text{var}(\boldsymbol{\varepsilon}_t) = \boldsymbol{\Sigma}_\varepsilon(t) = [\sigma_{i,i'}(t)]_{i,i'=1}^N$ with $\sigma_{i,i}(t) = 1$ for all i, i' and t . We denote the vector of parameters involved in modelling the within-panel conditional variance of $r_{i,t}$ by

$$\boldsymbol{\Omega}_i(t) = (\omega_i(t), \alpha_{i,1}(t), \dots, \alpha_{i,p}(t), \beta_{i,1}(t), \dots, \beta_{i,q}(t))^\top \in \mathbb{R}^{1+p+q},$$

and that involved in modelling the cross-correlations of $\varepsilon_{i,t}$ by

$$\boldsymbol{\Theta}_i(t) = (\sigma_{i,1}(t), \dots, \sigma_{i,i-1}(t), \sigma_{i,i+1}(t), \dots, \sigma_{i,N}(t))^\top \in \mathbb{R}^{N-1}.$$

Then, $\boldsymbol{\Omega}_i(t)$ and $\boldsymbol{\Theta}_i(t)$ are piecewise constant in t and share B change-points η_b , $b = 1, \dots, B$ (satisfying $0 \equiv \eta_0 < \eta_1 < \dots < \eta_B < \eta_{B+1} \equiv T$) across $i = 1, \dots, N$, in the sense that at any η_b , there exists $\Pi_b \subset \{(i, i') : 1 \leq i \leq i' \leq N\}$ with $|\Pi_b| \geq 1$, where $(i, i') \in \Pi_b$ iff either $\boldsymbol{\Omega}_i(\eta_b) \neq \boldsymbol{\Omega}_i(\eta_b + 1)$ (then $(i, i) \in \Pi_b$) or $\sigma_{i,i'}(\eta_b) \neq \sigma_{i,i'}(\eta_b + 1)$. Note that we do not require $|\Pi_b| = N(N+1)/2$, i.e., it is allowed that $\boldsymbol{\Omega}_i(t)$ or $\boldsymbol{\Theta}_i(t)$ corresponding to only a *subset* of the component time series undergo a change at each η_b .

In (1)–(2), we assume that the (unconditional) correlations across the components of \mathbf{r}_t are attributed to the correlations of $\boldsymbol{\varepsilon}_t$, and that the conditional variance within each component series is modelled separately as in the standard univariate GARCH processes. Thus, the tv-MGARCH model is reduced to the CCC model of [Bollerslev \(1990\)](#) over each stationary segment $[\eta_b + 1, \eta_{b+1}]$, since $\mathbb{E}(h_{i,t}^{-1/2} r_{i,t} h_{i',t}^{-1/2} r_{i',t} | \mathcal{F}_{t-1}) = \sigma_{i,i'}(\eta_b + 1)$. We take this approach with the aim of specifying the parameters to which structural changes may be introduced,

rather than the model for (possibly time-varying) conditional correlations between pairs of component series; it can be accomplished once the structural change-points are estimated and stationary segments are identified. We note that the literature on multivariate GARCH processes, as those cited in Introduction, considers a relatively lower-dimensional applications ($N \leq 8$), whereas we consider GARCH modelling of both simulated and real datasets of higher dimensions (N up to 100) in this paper.

We assume the following conditions on (1)–(2).

(A1) The dimensionality N satisfies $N \sim T^\theta$ for some $\theta \in [0, \infty)$.

(A2) For some $\epsilon_1 > 0$, $\Xi_1 < \infty$ and all T , we have

$$\min_{1 \leq i \leq N} \inf_{t \in \mathbb{Z}} \omega_i(t) > \epsilon_1 \text{ and } \max_{1 \leq i \leq N} \sup_{t \in \mathbb{Z}} \omega_i(t) \leq \Xi_1 < \infty.$$

(A3) For some $\epsilon_2 \in (0, 1)$ and all T , we have

$$\max_{1 \leq i \leq N} \sup_{t \in \mathbb{Z}} \left\{ \sum_{j=1}^p \alpha_{i,j}(t) + \sum_{k=1}^q \beta_{i,k}(t) \right\} \leq 1 - \epsilon_2.$$

Assumption (A1) indicates that the dimensionality can either be fixed or increase with T at a polynomial rate. Assumptions (A2)–(A3) guarantee that between any two consecutive change-points, each $r_{i,t}$ admits a well-defined solution a.s. and is weakly stationary (see e.g., Theorem 4.35 of Douc et al. (2014)).

For a non-stationary stochastic process X_t , its strong-mixing rate is defined as a sequence of coefficients

$$\alpha(k) = \sup_{t \in \mathbb{Z}} \sup_{\substack{G \in \sigma(X_{t+k}, X_{t+k+1}, \dots), \\ H \in \sigma(X_t, X_{t-1}, \dots)}} |\mathbb{P}(G \cap H) - \mathbb{P}(G)\mathbb{P}(H)|.$$

For BEKK multivariate GARCH models introduced in Engle and Kroner (1995), Theorem 2.4 of Boussama et al. (2011) shows that there exists a unique and strictly stationary solution, which is geometrically β -mixing and hence also strong mixing, i.e., $\alpha(k) \rightarrow 0$ as $k \rightarrow \infty$

with $\alpha(k) \sim \alpha^k$ for some $\alpha \in (0, 1)$. In [Fryzlewicz and Subba Rao \(2011\)](#) the mixing rate of univariate, time-varying ARCH processes was investigated. Adopting the theoretical tools of the latter paper, we establish that any pair of time-varying GARCH processes $\mathbf{r}_{i,i',t} = (r_{i,t}, r_{i',t})^\top$, $1 \leq i < i' \leq N$, is strong mixing at a geometric rate, under the following Lipschitz-type condition on the joint density of $(\varepsilon_{i,t}^2, \varepsilon_{i',t}^2)^\top$.

(A4) The joint distribution of $\varepsilon_{i,t}^2$ and $\varepsilon_{i',t}^2$, denoted by $f_{i,i'}(u, v)$, satisfies the following: for any $a > 0$, there exists fixed $K > 0$ independent of a such that

$$\left\{ \int \int |f_{i,i'}(u, v) - f_{i,i'}(u(1+a), v)| dudv \right\} \vee \left\{ \int \int |f_{i,i'}(u, v) - f_{i,i'}(u, v(1+a))| dudv \right\} \leq Ka$$

uniformly over $i, i' = 1, \dots, N$, $i \neq i'$.

Proposition 1. Under [\(A2\)](#)–[\(A4\)](#), there exists some $\alpha \in (0, 1)$ such that

$$\sup_{1 \leq i < i' \leq N} \sup_{\substack{G \in \sigma(\mathbf{r}_{i,i',u}: u \geq t+k), \\ H \in \sigma(\mathbf{r}_{i,i',u}: u \leq t)}} |\mathbb{P}(G \cap H) - \mathbb{P}(G)\mathbb{P}(H)| \leq M\alpha^k,$$

where M is a finite constant independent of t and k .

See [Appendix A.2](#) in the supplementary document for the proof.

3 Two-stage change-point detection methodology

3.1 Stage 1: Transformation of GARCH processes

For the segmentation of tv-MGARCH processes defined in [Section 2](#), we propose to transform \mathbf{r}_t into $d \equiv d_N = N(N+1)/2$ series such that any change in the conditional variance and correlations structure of \mathbf{r}_t , which is attributed to that in any of $\boldsymbol{\Omega}_i(t)$ or $\boldsymbol{\Theta}_i(t)$, is detectable as a change-point in the mean of at least one out of the d transformed series.

We first transform the N processes $r_{i,t}$ individually using a function $g_0 : \mathbb{R}^{1+p+q} \rightarrow \mathbb{R}$, which takes $\mathbf{r}_{i,t}^{t-p} = (r_{i,t}, \dots, r_{i,t-p})^\top$ and $\mathbf{h}_{i,t-1}^{t-q} = (h_{i,t-1}, \dots, h_{i,t-q})^\top$ as an input. We require that g_0 is bounded and Lipschitz continuous.

(A5) The function $g_0 : \mathbb{R}^{1+p+q} \rightarrow \mathbb{R}$ satisfies $|g_0| \leq \bar{g} < \infty$ and is Lipschitz continuous in its squared arguments, i.e., $|g_0(z_0, \dots, z_{p+q}) - g_0(z'_0, \dots, z'_{p+q})| \leq C_g \sum_{k=0}^{p+q} |z_k^2 - (z'_k)^2|$.

Empirical residuals have been widely adopted for detecting changes in the unconditional variance and/or parameters of univariate, conditionally heteroscedastic processes, see [Kokoszka and Teyssière \(2002\)](#), [Lee et al. \(2003\)](#), [De Pooter and Van Dijk \(2004\)](#), [Fryzlewicz and Subba Rao \(2014\)](#) and [Barassi et al. \(2018\)](#). For stationary processes, taking empirical residuals approximates a series of i.i.d. innovations and, even in the presence of change-points, such transformation tends to reduce the autocorrelations. Motivated by this, we select g_0 such that

$$\begin{aligned} U_{i,t} &= g_0(\mathbf{r}_{i,t}^{t-p}, \mathbf{h}_{i,t-1}^{t-q}) = \frac{r_{i,t}}{\sqrt{\check{h}_{i,t}}}, \quad \text{where} \\ \check{h}_{i,t} &= C_{i,0} + \sum_{j=1}^p C_{i,j} r_{i,t-j}^2 + \sum_{k=1}^q C_{i,p+k} h_{i,t-k} + \epsilon r_{i,t}^2. \end{aligned} \quad (3)$$

Following the practice adopted for the BASTA-res procedure of [Fryzlewicz and Subba Rao \(2014\)](#), we add $\epsilon r_{i,t}^2$ to $\check{h}_{i,t}$ with an arbitrary small positive constant ϵ , in order to ensure the boundedness of $U_{i,t}$. We note that other transformations may work well in place of g_0 , provided that they meet the conditions in (A5). When any parameter in $\boldsymbol{\Omega}_i(t)$ undergoes a shift over time, this change is expected to be reflected as a shift in $\mathbb{E}(U_{i,t}^2)$. More specifically,

$$U_{i,t}^2 = \frac{h_{i,t}}{\check{h}_{i,t}} \cdot \frac{r_{i,t}^2}{h_{i,t}} = \frac{h_{i,t}}{\check{h}_{i,t}} \varepsilon_{i,t}^2 = \frac{h_{i,t}}{\check{h}_{i,t}} + \frac{h_{i,t}}{\check{h}_{i,t}} (\varepsilon_{i,t}^2 - 1), \quad (4)$$

so that $U_{i,t}^2$ contains any change in $\boldsymbol{\Omega}_i(t)$ as a change in its level. Choices of the parameters $C_{i,j}$, $j = 0, \dots, p+q$ and the treatment of (unobservable) $h_{i,t}$ are discussed in [Section 3.3](#). For notational convenience, we define

$$g_1(\mathbf{r}_{i,t}^{t-p}, \mathbf{h}_{i,t-1}^{t-q}) = \{g_0(\mathbf{r}_{i,t}^{t-p}, \mathbf{h}_{i,t-1}^{t-q})\}^2 = U_{i,t}^2 = \frac{r_{i,t}^2}{\check{h}_{i,t}}.$$

To capture any changes in the cross-sectional dependence structure of \mathbf{r}_t , we adopt the

transformation $g_2 : \mathbb{R}^{2+2p+2q} \rightarrow \mathbb{R}$:

$$U_{ii',t} = g_2(\mathbf{r}_{i,t}^{t-p}, \mathbf{h}_{i,t-q}, \mathbf{r}_{i',t}^{t-p}, \mathbf{h}_{i',t-q}) = (U_{i,t} - s_{i,i'} U_{i',t})^2$$

where $s_{i,i'} \in \{1, -1\}$ denotes the choice of a ‘sign’ to which our methodology is blind theoretically; we defer the discussion on its empirical choice to Section 3.3. Under Assumption (A5), g_2 is also bounded and Lipschitz continuous in its squared arguments (see Appendix A.5 of the supplementary document). Similarly to (4), $U_{ii',t}$ is decomposed as

$$U_{ii',t} = \frac{h_{i,t}}{h_{i,t}} + \frac{h_{i,t}}{h_{i,t}}(\varepsilon_{i,t}^2 - 1) + \frac{h_{i',t}}{h_{i',t}} + \frac{h_{i',t}}{h_{i',t}}(\varepsilon_{i',t}^2 - 1) - 2s_{i,i'} \sqrt{\frac{h_{i,t}h_{i',t}}{h_{i,t}h_{i',t}}} \varepsilon_{i,t}\varepsilon_{i',t}$$

from which we conclude that a change in $\sigma_{i,i'}(t)$ are detectable from $U_{ii',t}$ as that in its level.

Regarding $U_{i,t}$ as empirical residuals obtained by applying volatility filters, the change-point procedure of Andreou and Ghysels (2003) examines $U_{1,t}U_{2,t}$, $U_{1,t}^2U_{2,t}^2$ and $|U_{1,t}U_{2,t}|$ for detecting structural changes in the co-movement of a pair of series $(r_{1,t}, r_{2,t})^\top$. Instead, we adopt $U_{ii',t}$, whose formulation is motivated by the observation made in Cho and Fryzlewicz (2015): for given (a_t, b_t) , any changes in the second-order dependence structure, $\mathbb{E}(a_t^2)$, $\mathbb{E}(b_t^2)$ and $\mathbb{E}(a_t b_t)$, are detectable by jointly examining $\mathbb{E}(a_t^2)$, $\mathbb{E}(b_t^2)$ and $\mathbb{E}\{(a_t - s_{a,b}b_t)^2\}$ for any $s_{a,b} \in \{1, -1\}$. More importantly, we can regard $U_{ii',t}$ on an equal footing with $U_{i,t}^2$ and $U_{i',t}^2$, which is essential in accomplishing the simultaneous segmentation of \mathbf{r}_t according to both within-series and cross-sectional dependence structure. Under the stationarity, the choice of $C_{i,0} = \omega_i$, $C_{i,j} = \alpha_{i,j}$ and $C_{i,p+k} = \beta_{i,k}$ leads to $U_{i,t}^2$ closely approximating $\varepsilon_{i,t}^2$, while $U_{ii',t}$ approximates $(\varepsilon_{i,t} - s_{i,i'}\varepsilon_{i',t})^2$. Upon further imposing Gaussianity on $\varepsilon_{i,t}$, all $U_{i,t}$ and $U_{ii',t}$ follow a scaled χ_1^2 distribution (approximately). Note that the same arguments do not apply to the transformations adopted by Andreou and Ghysels (2003).

In summary, we transform the N -dimensional time series \mathbf{r}_t to the d -dimensional panel data with $d = N(N + 1)/2$, as

$$\{U_{i,t}^2, 1 \leq i \leq N, U_{ii',t}, 1 \leq i < i' \leq N; 1 \leq t \leq T\}, \quad (5)$$

which ‘encode’ any changes in $\boldsymbol{\Omega}_i(t)$ and $\boldsymbol{\Theta}_i(t)$, $i = 1, \dots, N$ as changes in their levels. Then, the problem of detecting multiple change-points in the more complex dependence structure of \mathbf{r}_t , is transformed into a relatively easier problem of detecting change-points in the means of the panel data. While this also brings the increase of dimensionality, the panel data segmentation algorithm adopted in the second stage (detailed in Section 3.2) handles the high dimensionality well under a mild assumption (A1).

To formalise the above observations, we introduce the following notations. For each $b = 1, \dots, B$, let $\{\mathbf{r}_t^b\}_{t=1}^T$ denote a stationary multivariate GARCH(p, q) process that follows (1)–(2) with the parameters $\boldsymbol{\Omega}_i(\eta_b + 1)$, $\boldsymbol{\Theta}_i(\eta_b + 1)$ and $\boldsymbol{\Sigma}_\varepsilon(\eta_b + 1)$, and the innovations coinciding with ε_t over the associated segment $[\eta_b + 1, \eta_{b+1}]$; we denote the corresponding conditional variance by \mathbf{h}_t^b . Then, we define $\tilde{U}_{i,t}^b = g_0(\mathbf{r}_{i,t}^{b,t-p}, \mathbf{h}_{i,t-1}^{b,t-q})$ and $\tilde{U}_{ii',t}^b = g_2(\mathbf{r}_{i,t}^{b,t-p}, \mathbf{h}_{i,t-1}^{b,t-q}, \mathbf{r}_{i',t}^{b,t-p}, \mathbf{h}_{i',t-1}^{b,t-q})$, which are constructed similarly to $U_{i,t}$ and $U_{ii',t}$ yet with stationary \mathbf{r}_t^b and \mathbf{h}_t^b . Finally, we denote the index of the change-point strictly to the left of and nearest to t by $v(t) = \max\{0 \leq b \leq B : \eta_b < t\}$, with which piecewise stationary processes $\mathbf{r}_t^{v(t)}$, $\mathbf{h}_t^{v(t)}$, $\tilde{U}_{i,t}^{v(t)}$ and $\tilde{U}_{ii',t}^{v(t)}$ are defined.

Proposition 2. Suppose that (A2)–(A5) hold, and let $x_{j,t}$ denote an element of the d -dimensional panel data in (5), i.e., $x_{j,t} = U_{ii',t}$ for $j \equiv j(i, i') = (N - i/2)(i - 1) + i'$ (with $U_{ii,t} \equiv U_{i,t}^2$ for notational convenience), $1 \leq i \leq i' \leq N$. Then, we have the following decomposition

$$x_{j,t} = f_{j,t} + z_{j,t}, \quad 1 \leq j \leq d; \quad 1 \leq t \leq T. \quad (6)$$

- (i) $f_{j,t}$ are piecewise constant as $f_{j,t} = \tilde{g}_{ii',t}$ (with $\tilde{g}_{ii,t} \equiv \tilde{g}_{i,t}$), where $\tilde{g}_{i,t} = \mathbb{E}\{(\tilde{U}_{i,t}^{v(t)})^2\}$ and $\tilde{g}_{ii',t} = \mathbb{E}(\tilde{U}_{ii',t}^{v(t)})$. All change-points in $f_{j,t}$ belong to $\mathcal{B} = \{\eta_1, \dots, \eta_B\}$ and, conversely, for each $\eta_b \in \mathcal{B}$, there exists at least a single index $j \in \{1, \dots, d\}$ for which $|z_{j,\eta_b+1} - z_{j,\eta_b}| \neq 0$.
- (ii) $z_{j,t}$ satisfies

$$\max_{1 \leq j \leq d} \max_{1 \leq s < e \leq T} \frac{1}{\sqrt{e - s + 1}} \left| \sum_{t=s}^e z_{j,t} \right| = O_p(\sqrt{\log T}).$$

Proof of Proposition 2 can be found in Appendix A.3 of the supplementary document.

Unlike $\mathbb{E}(U_{i,t}^2)$ or $\mathbb{E}(U_{ii',t})$, we have $\tilde{g}_{i,t}$ and $\tilde{g}_{ii',t}$ *exactly* constant between any two adjacent change-points without any boundary effects. By its construction, $z_{j,t} = U_{ii',t} - \mathbb{E}(\tilde{U}_{ii',t}^{v(t)})$ does not satisfy $\mathbb{E}(z_{j,t}) = 0$. However, due to the mixing properties of $U_{ii',t}$ derived from Proposition 1, its scaled partial sums can be appropriately bounded. In the next section, we introduce the multiple change-point detection algorithm as that applied to the panel data $x_{j,t}$ in (6).

3.2 Stage 2: Binary segmentation for tv-MGARCH processes

In this section, we introduce the second stage of the proposed methodology which simultaneously segments the d -dimensional transformation of \mathbf{r}_t , as applied to the additive panel data in (6).

3.2.1 Double CUSUM binary segmentation

We first describe the Double CUSUM statistics computed on a generic segment $[s, e]$ for some $1 \leq s < e \leq T$, and then provide a full description of the Double CUSUM binary segmentation algorithm.

Cumulative sum (CUSUM) statistics have been widely adopted for change-point detection in both univariate and multivariate data. We adopt the (weighted) CUSUM statistics, which is defined as

$$\mathcal{X}_{s,c,e}^j = \sqrt{\frac{(c-s+1)(e-c)}{e-s+1}} \left(\frac{1}{c-s+1} \sum_{t=s}^c x_{j,t} - \frac{1}{e-c} \sum_{t=c+1}^e x_{j,t} \right) \text{ for } s \leq c < e. \quad (7)$$

A large value of $|\mathcal{X}_{s,c,e}^j|$ typically indicates the presence of a change-point in the level of $x_{j,t}$ in the vicinity of $t = c$, and the asymptotic properties of the CUSUM-based test statistic have been studied for testing the presence of a single change-point, see e.g., [Csörgö and Horváth \(1997\)](#). Combined with the binary segmentation algorithm, the CUSUM statistic has frequently been adopted to multiple change-point detection in univariate time series; see [Vostrikova \(1981\)](#) and [Venkatraman \(1992\)](#) for the theoretical treatment of its application to the canonical additive model with independent noise, and [Fryzlewicz and Subba Rao \(2014\)](#) for its application to segment piecewise stationary ARCH processes.

For change-point detection in multivariate data, we may apply univariate change-point detection procedures to each $x_{j,t}$ separately as suggested by [Andreou and Ghysels \(2003\)](#), and then prune down the estimated change-points cross-sectionally. However, identification of common change-points is a challenging task even for moderately large d , due to the bias in change-point estimators. Moreover, such an approach does not exploit the cross-sectional nature of the change-points, that they may be shared cross-sectionally, which advocates the simultaneous segmentation of the panel data.

We adopt the Double CUSUM Binary Segmentation (DCBS) algorithm proposed in [Cho \(2016\)](#) for multiple change-point detection in the high-dimensional panel data. It guarantees consistency in estimating both the number and locations of multiple change-points while permitting both serial and cross-sectional correlations in $x_{j,t}$, which is highly relevant to the time series setting studied in this paper. The Double CUSUM (DC) statistics are computed on the CUSUM statistics $\mathcal{X}_{s,c,e}^j$ and form a two-dimensional array of DC statistics as

$$\mathcal{D}_{s,e}(c, m) = \sqrt{\frac{m(2d-m)}{2d}} \left(\frac{1}{m} \sum_{j=1}^m |\mathcal{X}_{s,c,e}^{(j)}| - \frac{1}{2d-m} \sum_{j=n+1}^d |\mathcal{X}_{s,c,e}^{(j)}| \right) \quad (8)$$

for $s \leq c < e$ and $1 \leq m \leq d$, where $|\mathcal{X}_{s,c,e}^{(j)}|$ denote the ordered CUSUM statistics at each c such that $|\mathcal{X}_{s,c,e}^{(1)}| \geq |\mathcal{X}_{s,c,e}^{(2)}| \geq \dots \geq |\mathcal{X}_{s,c,e}^{(d)}|$. Then, the test statistic is derived by maximising the two-dimensional array over both time and cross-sectional indices, as

$$\mathcal{T}_{s,e} = \max_{s \leq c < e} \max_{1 \leq m \leq d} \mathcal{D}_{s,e}(c, m), \quad (9)$$

which is compared against a threshold, $\pi_{d,T}$, for determining the presence of a change-point over the interval $[s, e]$. If $\mathcal{T}_{s,e} > \pi_{d,T}$, the location of the change-point is estimated as

$$\hat{\eta} = \arg \max_{s \leq c < e} \max_{1 \leq m \leq d} \mathcal{D}_{s,e}(c, m).$$

By ordering the cross-sectional CUSUMs and taking maximum over both the time and cross-sectional dimensions, we not only locate the change-points over time, but also identify those

cross-sections that contribute to the detection of the change-point by containing large changes in the level of $x_{j,t}$, in a data-driven way with respect to

$$\hat{m} = \arg \max_{1 \leq m \leq d} \mathcal{D}_{s,e}(\hat{\eta}, m);$$

that is, those $x_{j,t}$ corresponding to $|\mathcal{X}_{s,c,e}^{(l)}|$, $l \leq \hat{m}$ are the cross-sectional components that contribute to the large value of $\mathcal{T}_{s,e}$.

Remark 1. We briefly remark upon the choice of scaling for the DC statistics in (8), namely $\sqrt{m(2d-m)/(2d)}$ in place of $\sqrt{m(d-m)/d}$. While the latter is in line with the scaling adopted for the weighted CUSUM statistic in (7), when applied to the cross-sectional dimension, it does not favour a change-point shared by more than $d/2$ rows of the panel data and actually acts as a penalty when all d rows share a change-point, which is counter-intuitive. The choice of the former scaling resolves this issue, and favourably regards the ‘density’ of a change-point in considering its cross-sectional magnitude.

The DCBS algorithm is formulated in Algorithm 1. Initialised with $s = 1$, $e = T$ and $\hat{\mathcal{B}} = \emptyset$, it recursively performs testing for locating a single change-point over the segments defined by previously detected change-points until they are no longer partitioned according to the threshold $\pi_{d,T}$. We discuss the choice of $\pi_{d,T}$ in Section 3.4.

Algorithm 1: DCBinSeg (Double CUSUM Binary Segmentation algorithm)

Input: $\{x_{j,t}\}$, $\pi_{d,T}$, s , e , $\hat{\mathcal{B}}$

Step 1: compute $\mathcal{D}_{s,e}(c, m)$ for $s \leq c < e$ and $1 \leq m \leq d$

Step 2: set

$$\mathcal{T}_{s,e} \leftarrow \max_{s \leq c < e} \max_{1 \leq m \leq d} \mathcal{D}_{s,e}(c, m) \text{ and } \hat{\eta} \leftarrow \arg \max_{s \leq c < e} \max_{1 \leq m \leq d} \mathcal{D}_{s,e}(c, m)$$

Step 3: if $\mathcal{T}_{s,e} > \pi_{d,T}$ then

$\hat{\mathcal{B}} \leftarrow \hat{\mathcal{B}} \cup \{\hat{\eta}\}$
 $\hat{\mathcal{B}} \leftarrow \text{DCBinSeg}(\{x_{j,t}\}, \pi_{d,T}, s, \hat{\eta}, \hat{\mathcal{B}})$
 $\hat{\mathcal{B}} \leftarrow \text{DCBinSeg}(\{x_{j,t}\}, \pi_{d,T}, \hat{\eta} + 1, e, \hat{\mathcal{B}})$

end

Output: $\hat{\mathcal{B}}$

3.2.2 Theoretical properties of DCBS algorithm

Recall Proposition 2 (i), which shows that piecewise constant signals $\{f_{j,t}\}_{t=1}^T$, $j = 1, \dots, d$ contain the B change-points η_b , $b = 1, \dots, B$ shared by the vectors of piecewise constant parameters $\mathbf{\Omega}_i(t)$ and $\mathbf{\Theta}_i(t)$, $i = 1, \dots, N$ and, conversely, at each η_b , there exists

$$\tilde{\Pi}_b = \left\{ j : \Delta_{j,b} := |f_{j,\eta_{b+1}} - f_{j,\eta_b}| \neq 0 \right\} \subset \{1, \dots, d\}$$

with $|\tilde{\Pi}_b| \geq 1$. In order to establish the theoretical consistency of the DCBS algorithm, we impose the following conditions chiefly on the quantities that control the detectability of each change-point η_b .

- (B1) There exists a fixed constant $\bar{f} > 0$ such that $\max_{1 \leq j \leq d} \max_{1 \leq t \leq T} |f_{j,t}| \leq \bar{f}$.
- (B2) There exists a fixed constant $c > 0$ such that $\min_{0 \leq b \leq B} (\eta_{b+1} - \eta_b) \geq cT^\gamma$ for some $\gamma \in (6/7, 1]$ (with $\eta_0 = 0$ and $\eta_{B+1} = T$).
- (B3) The number of change-points, $B \equiv B_T$, satisfies $B = o(\log T)$.
- (B4) We have $\underline{\Delta}_{d,T} = \min_{1 \leq b \leq B} |\tilde{\Pi}_b|^{-1/2} \sum_{j \in \tilde{\Pi}_b} \Delta_{j,b}$ satisfy $T^{7\gamma/4-3/2} \underline{\Delta}_{d,T} / \sqrt{d \log T} \rightarrow \infty$ as $T \rightarrow \infty$.

The condition in (B1) holds trivially as a consequence of (A5). In general, change-point detection becomes more challenging as the distance between two adjacent change-points decreases. This is reflected on (B2), which still allows the case where $T^{-1}(\eta_{b+1} - \eta_b) \rightarrow 0$ as $T \rightarrow \infty$. In conjunction with (B2), Assumption (B3) imposes a bound on the total number of change-points B , which is permitted to grow slowly with T . Assumption (B4) specifies the minimum requirement on the *cross-sectional size of the change*, quantified by $\underline{\Delta}_{d,T}$, for all the change-points to be detected as well as being located with accuracy. The quantity $\underline{\Delta}_{d,T}$ combines both the density, $|\tilde{\Pi}_b|$, and the magnitude of jumps, $\sum_{j \in \tilde{\Pi}_b} \Delta_{j,b}$, over all $b = 1, \dots, B$, and tends to increase as both quantities increase. We highlight that our methodology does not require each change-point to be common to all the cross-sections of $\{z_{j,t}\}$ (and, consequently, in all $\mathbf{\Omega}_i(t)$ and $\mathbf{\Theta}_i(t)$) provided that Assumption (B4) is met. It is not trivial to relate the

magnitude of a jump in $f_{j,t} = \tilde{g}_{i' t} = \mathbb{E}\{(U_{i' t}^{v(t)})^2\}$ (with $j = (N - i/2)(i - 1) + i'$) and the changes in $\Omega_i(t)$ or $\Theta_i(t)$ due to the presence of the complex transformation. However, the density or sparsity of a change-point, measured by $|\Pi_b|$ (defined in Section 2), is preserved by $|\tilde{\Pi}_b|$ and, in fact, $(i, i') \in \Pi_b$ iff $j = (N - i/2)(i - 1) + i' \in \tilde{\Pi}_b$. For a detailed discussion on the high-dimensional efficiency of DC test statistic, see Remark 3 of Cho (2016).

Theorem 1. Let $\hat{\eta}_b$, $b = 1, \dots, \hat{B}$ ($1 < \hat{\eta}_1 < \dots < \hat{\eta}_{\hat{B}} < T$) denote the change-points estimated by the DCBS algorithm with a test criterion $\pi_{d,T}$. Assume that (A1)–(A5) and (B1)–(B4) hold and $\pi_{d,T}$ satisfies $C' d \underline{\Delta}_{d,T}^{-1} T^{5(1-\gamma)/2} \sqrt{\log T} < \pi_{d,T} < C'' \underline{\Delta}_{d,T} T^{\gamma-1/2}$ for some constants $C', C'' > 0$. Then there exists $c_0 > 0$ such that

$$\mathbb{P} \left\{ \hat{B} = B; |\hat{\eta}_b \mathbb{I}(b \leq \hat{B}) - \eta_b| < c_0 \epsilon_T \text{ for } b = 1, \dots, B \right\} \rightarrow 1$$

as $T \rightarrow \infty$, where $\epsilon_T = d \underline{\Delta}_{d,T}^{-2} T^{5(1-\gamma)} \log T$.

For the proof of Theorem 1, see Appendix A.4 of the supplementary document. From the condition imposed on the rate of $\underline{\Delta}_{d,T}$ in (B4), it is easily seen that $\epsilon_T/T^\gamma \rightarrow 0$ as $T \rightarrow \infty$. That is, in the re-scaled time interval $[0, 1]$, the change-point estimators satisfy $T^{-1}|\hat{\eta}_b - \eta_b| \leq T^{-\gamma}|\hat{\eta}_b - \eta_b| \rightarrow 0$ for all $b = 1, \dots, B$. Defining the optimality in change-point detection as when each of the true change-points and the corresponding estimated change-point are within the distance of $O_p(1)$ (see e.g., Korostelev (1987)), it is attained up to a logarithmic factor when the change-points are maximally spread ($\gamma = 1$), and the jumps are dense ($|\tilde{\Pi}_b| \sim d$) and of large magnitude ($\sum_{j \in \tilde{\Pi}_b} \Delta_{j,b} \sim d$).

3.3 Choice of parameters for transformation

Empirical performance of the two-stage methodology, its power in particular, is influenced by the choice of the transformation function g_0 determined by the coefficients $C_{i,j}$, $j = 0, \dots, p+q$. As in many references given at the beginning of Section 3.1, we may replace $C_{i,j}$ in (3) with the maximum likelihood estimates (MLEs) of the GARCH parameters obtained assuming the stationarity, say $\hat{\omega}_i, \hat{\alpha}_{i,j}$, $1 \leq j \leq p$ and $\hat{\beta}_{i,k}$, $1 \leq k \leq q$.

The BASTA-res algorithm proposed by [Fryzlewicz and Subba Rao \(2014\)](#) performs change-point detection in the univariate GARCH process by analysing the transformation of the input time series obtained similarly to $U_{i,t}^2$. They recommend the use of ‘dampened’ versions of the GARCH parameter estimates. In our setting, this leads to the choice of $C_{i,0} = \hat{\omega}_i$, $C_{i,j} = \hat{\alpha}_{i,j}/F_i$, $1 \leq j \leq p$ and $C_{i,p+k} = \hat{\beta}_{i,k}/F_i$, $1 \leq k \leq q$, with within-series dampening parameters $F_i \geq 1$.

Empirically, the motivation behind the introduction of F_i is as follows. For $r_{i,t}$ with time-varying parameters, we often observe that $\alpha_{i,j}$ and $\beta_{i,k}$ are over-estimated such that $\sum_{j=1}^p \hat{\alpha}_{i,j} + \sum_{k=1}^q \hat{\beta}_{i,k}$ is close to, or even exceeds, one. Therefore, using the raw estimates in place of $C_{i,j}$ ’s in (3) leads to $U_{i,t}$ where any change in $\mathbb{E}(U_{i,t}^2)$ induced by a change-point in $\Omega_i(t)$ tends to be attenuated. Hence we adopt the dampening parameter F_i which is chosen as

$$F_i = \max \left[1, \frac{\min(0.99, \sum_{j=1}^p \hat{\alpha}_{i,j} + \sum_{k=1}^q \hat{\beta}_{i,k})}{\max \{0.01, 1 - (\sum_{j=1}^p \hat{\alpha}_{i,j} + \sum_{k=1}^q \hat{\beta}_{i,k})\}} \right].$$

By construction, F_i is bounded as $F_i \in [1, 99]$ and approximately brings $\hat{\omega}_i$ and $\sum_{j=1}^p \hat{\alpha}_{i,j} + \sum_{k=1}^q \hat{\beta}_{i,k}$ to the same scale.

Also, the transformation g_0 involves the unobservable conditional variance $h_{i,t}$, which we propose to replace with the empirical estimates

$$\hat{h}_{i,t} = \hat{\omega}_i + \sum_{j=1}^p \hat{\alpha}_{i,j} r_{i,t-j}^2 + \sum_{k=1}^q \hat{\beta}_{i,k} \hat{h}_{i,t-k} \quad (10)$$

obtained with the MLE estimates of the GARCH parameters.

Typically, the GARCH orders p and q are unknown and may even vary over time. We propose to use $(p, q) = (1, 1)$. The GARCH(1, 1) model is simple yet known to provide a good fit to wide range of datasets (see e.g., [Hansen and Lunde \(2005\)](#)). We note that the transformation g_0 is adopted for change-point analysis, rather than for accurate modelling of the time series; once all the change-points are consistently estimated, we can adopt a more sophisticated modelling approach to each segment. In simulation studies reported in

Section 4, we study the effect of mis-specifying the GARCH orders on change-point analysis, which shows that the choice of $(p, q) = (1, 1)$ works well even when it under-specifies the true GARCH orders.

Theoretically, both choices of $s_{i,i'} \in \{1, -1\}$ within the transformation g_2 are valid for detecting change-points in $\mathbb{E}(U_{i,t}U_{i',t})$. However, its choice may influence the finite sample performance in the sense that one value results in a transformed series that reveals the structural changes better than the other. Based on the observations made in [Cho and Fryzlewicz \(2015\)](#), we adopt the choice $s_{i,i'} = \text{sign}(\widehat{\text{corr}}_{s,e}(U_{i,t}, U_{i',t}))$, where $[s, e]$ denotes any segment considered by the binary segmentation as it progresses (see [Algorithm 1](#)), and $\widehat{\text{corr}}_{s,e}$ the sample correlation computed over a segment $[s, e]$.

3.4 Choice of threshold for DCBS algorithm

[Theorem 1](#) provides a range for the rate of $\pi_{d,T}$ that returns consistent estimation of multiple change-points. However, the theoretical range involves typically unattainable knowledge on the quantities such as γ or $\underline{\Delta}_{d,T}$. Moreover, even when such knowledge is available, finite sample performance may be affected by the choice of the multiplicative constant to the given rate. Instead, we propose a parametric resampling procedure, which enables us to approximate the distribution of DC test statistic in the presence of no change-points. A similar approach has widely been adopted in the change-point literature including [Kokoszka and Teyssière \(2002\)](#) in the context of testing the presence of a change-point in the parameters of univariate GARCH models. [Algorithm 2](#) outlines the proposed resampling scheme, where we derive the segment-dependent threshold $\pi_{d,T}^{(s,e)}$ for each segment $[s, e]$ considered at some iteration of the DCBS algorithm (see [Algorithm 1](#)).

Algorithm 2: Bootstrap algorithm for threshold selection

Input: $\{r_{i,t}\}, \{\hat{h}_{i,t}\}$ (see (10)), $s, e, R, g_1, g_2, \alpha$

Step 1: compute the empirical residuals $\hat{\varepsilon}_{i,t} \leftarrow \hat{h}_{i,t}^{-1/2} r_{i,t}$

Step 2: for $\ell = 1, \dots, R$ do

Step 2.1: generate bootstrap samples $\{\boldsymbol{\varepsilon}_t^\ell\}_{t=1}^T$ of $\{\hat{\boldsymbol{\varepsilon}}_t = (\hat{\varepsilon}_{1,t}, \dots, \hat{\varepsilon}_{N,t})^\top\}_{t=1}^T$

Step 2.2: simulate the MGARCH process

$$r_{i,t}^\ell = (h_{i,t}^\ell)^{1/2} \varepsilon_{i,t}^\ell, \quad \text{where} \quad h_{i,t}^\ell = \hat{\omega}_i + \sum_{j=1}^p \hat{\alpha}_{i,j} (r_{i,t-j}^\ell)^2 + \sum_{k=1}^q \hat{\beta}_{i,k} h_{i,t-k}^\ell$$

Step 2.3: generate $\{x_{j,t}^\ell\}$ as

$$\left\{ g_1(\mathbf{r}_{i,t}^{\ell,t-p}, \mathbf{h}_{i,t-1}^{\ell,t-q}), 1 \leq i \leq N, g_2(\mathbf{r}_{i,t}^{\ell,t-p}, \mathbf{h}_{i,t-1}^{\ell,t-q}, \mathbf{r}_{i',t}^{\ell,t-p}, \mathbf{h}_{i',t-1}^{\ell,t-q}), 1 \leq i < i' \leq N; 1 \leq t \leq T \right\}$$

Step 2.3: calculate $\mathcal{T}_{s,e}^\ell$ from $\{x_{j,t}^\ell\}$ as in (9)

end

Step 3: select $\pi_{d,T}^{(s,e)}$ as the $100(1 - \alpha)\%$ -percentile of $\mathcal{T}_{s,e}^\ell$, $\ell = 1, \dots, R$

Output: $\pi_{d,T}^{(s,e)}$

4 Simulation study

4.1 Models

We study the change-point detection consistency of the two-stage change-point detection methodology described in Section 3 on the datasets simulated from the following models. The choices of parameters for (M0)–(M1) are considered in Fryzlewicz and Subba Rao (2014), while those for (M2)–(M3) are considered in Kokoszka and Teysnière (2002), in the context of *single* change-point test in *univariate* GARCH processes.

(M0) **Stationary MGARCH (1, 1) processes.** Let $\omega_i = \omega + \delta_{\omega,i}$, $\alpha_{i,1} = \alpha + \delta_{\alpha,i}$ and $\beta_{i,1} = \beta + \delta_{\beta,i}$, where $\delta_{\cdot,1} \stackrel{iid}{\sim} \mathcal{U}(-\Delta, \Delta)$ for some small $\Delta > 0$ is added to each GARCH parameter so that every $r_{i,t}$ has a slightly different set of GARCH parameters. The innovations are generated from two different distributions, namely (i) $\boldsymbol{\varepsilon}_t \stackrel{i.i.d}{\sim} \mathcal{N}(\mathbf{0}, \boldsymbol{\Sigma}_\varepsilon)$ where $\sigma_{i,i'} = \rho^{|i-i'|}$ with $\rho = -0.75$ and (ii) $\varepsilon_{i,t} \stackrel{i.i.d}{\sim} t_{10}$ for each i and t . We consider $T = 1000$ and $N \in \{50, 100\}$.

(M0.1) $(\omega, \alpha_1, \beta_1) = (0.4, 0.1, 0.5)$.

$$(M0.2) \quad (\omega, \alpha_1, \beta_1) = (0.1, 0.1, 0.8).$$

(M1) **tv-MGARCH (1, 1) processes with a single change-point.** Change-points are introduced to GARCH parameters in (1)–(2) at $\eta_1 \in \{[T/2], [0.9T]\}$, where $T = 1000$ and $N \in \{50, 100\}$. For a randomly chosen $i \in \mathcal{S}_1 \subset \{1, \dots, N\}$, GARCH parameters $\omega_i(t)$, $\alpha_{i,1}(t)$ and $\beta_{i,1}(t)$ for $i \in \mathcal{S}_1$ change at $t = \eta_1$ as $\omega_i(t) = \omega^{(1)}\mathbb{I}(t \leq \eta_1) + \omega^{(2)}\mathbb{I}(t > \eta_1) + \delta_{\omega,i}$, $\alpha_{i,1}(t) = \alpha_1^{(1)}\mathbb{I}(t \leq \eta_1) + \alpha_1^{(2)}\mathbb{I}(t > \eta_1) + \delta_{\alpha,i}$ and $\beta_{i,1}(t) = \beta_1^{(1)}\mathbb{I}(t \leq \eta_1) + \beta_1^{(2)}\mathbb{I}(t > \eta_1) + \delta_{\beta,i}$, where $|\mathcal{S}_1| = [\varrho N]$ with $\varrho \in \{1, 0.75, 0.5, 0.25\}$ controlling the ‘sparsity’ of the change-point. We have $\delta_{\cdot,i} \stackrel{\text{i.i.d.}}{\sim} \mathcal{U}(-\Delta, \Delta)$ is as in (M0), and $\boldsymbol{\varepsilon}_t \sim \mathcal{N}(\mathbf{0}, \boldsymbol{\Sigma}_\varepsilon(t))$ with $\boldsymbol{\Sigma}_\varepsilon(t) = \boldsymbol{\Sigma}_\varepsilon$ defined in (M0).

$$(M1.1) \quad (\omega, \alpha_1, \beta_1) : (0.4, 0.1, 0.5) \rightarrow (0.4, 0.1, 0.6).$$

$$(M1.2) \quad (\omega, \alpha_1, \beta_1) : (0.4, 0.1, 0.5) \rightarrow (0.4, 0.1, 0.8).$$

$$(M1.3) \quad (\omega, \alpha_1, \beta_1) : (0.1, 0.1, 0.8) \rightarrow (0.1, 0.1, 0.7).$$

$$(M1.4) \quad (\omega, \alpha_1, \beta_1) : (0.1, 0.1, 0.8) \rightarrow (0.1, 0.1, 0.4).$$

$$(M1.5) \quad (\omega, \alpha_1, \beta_1) : (0.4, 0.1, 0.5) \rightarrow (0.5, 0.1, 0.5).$$

$$(M1.6) \quad (\omega, \alpha_1, \beta_1) : (0.4, 0.1, 0.5) \rightarrow (0.8, 0.1, 0.5).$$

$$(M1.7) \quad (\omega, \alpha_1, \beta_1) : (0.1, 0.1, 0.8) \rightarrow (0.3, 0.1, 0.8).$$

$$(M1.8) \quad (\omega, \alpha_1, \beta_1) : (0.1, 0.1, 0.8) \rightarrow (0.5, 0.1, 0.8).$$

(M2) **tv-MGARCH (1, 1) processes with two change-points.** We introduce the first change-point $\eta_1 = [T/4]$ to the GARCH parameters as in (M1), where:

$$(M2.1) \quad (\omega, \alpha_1, \beta_1) : (0.1, 0.3, 0.3) \rightarrow (0.15, 0.25, 0.65).$$

$$(M2.2) \quad (\omega, \alpha_1, \beta_1) : (0.1, 0.3, 0.3) \rightarrow (0.125, 0.1, 0.6).$$

$$(M2.3) \quad (\omega, \alpha_1, \beta_1) : (0.1, 0.3, 0.3) \rightarrow (0.15, 0.15, 0.25).$$

Also, a change-point is introduced to $\boldsymbol{\Sigma}_\varepsilon(t)$ at $\eta_2 = [3T/5]$ as below. Initially, $\boldsymbol{\varepsilon}_t \sim \mathcal{N}(\mathbf{0}, \boldsymbol{\Sigma}_\varepsilon(t))$ with $\boldsymbol{\Sigma}_\varepsilon(t) = \boldsymbol{\Sigma}_\varepsilon$ defined in (M0) up to $t = \eta_2$. Then, for a randomly chosen $i \in \mathcal{S}_2 \subset \{1, \dots, N\}$, rows of $\boldsymbol{\Sigma}_\varepsilon(t)$ corresponding to such $\varepsilon_{i,t}$ swap their locations

arbitrarily. We set $|\mathcal{S}_1| = |\mathcal{S}_2| = \lceil \varrho N \rceil$ with $\varrho \in \{1, 0.75, 0.5, 0.25\}$, and consider the sample size $T = 500$ and $N \in \{50, 100\}$.

(M3) **Mis-specification of the orders p and q .**

(M3.1) Over-specification. The two change-points are introduced to tv-MGARCH(1, 1) processes as in (M2.1)–(M2.2) (referred to as (M3.1.1)–(M3.1.2)), but the GARCH orders are mis-specified in Stage 1 as $(p, q) = (2, 2)$.

(M3.2) Under-specification. The two change-points are introduced to tv-MGARCH(2, 2) processes as in (M2), with the GARCH parameters change at η_1 as:

$$(M3.2.1) \quad (\omega, \alpha_1, \alpha_2, \beta_1, \beta_2): (0.1, 0.1, 0.2, 0.1, 0.2) \rightarrow (0.15, 0.15, 0.1, 0.35, 0.3); \text{ or}$$

$$(M3.2.2) \quad (\omega, \alpha_1, \alpha_2, \beta_1, \beta_2): (0.1, 0.1, 0.2, 0.1, 0.2) \rightarrow (0.125, 0.1, 0, 0.3, 0.3).$$

The covariance matrix of the innovations change at η_2 as in (M2). The GARCH orders are mis-specified in Stage 1 as $(p, q) = (1, 1)$.

(M4) **Full-factor multivariate GARCH(1, 1) model with time-varying factors and loadings.** Proposed in [Vrontos et al. \(2003\)](#), each $r_{i,t}$ is generated as a linear combination of the independent factors $f_{j,t}$, $j = 1, \dots, N$ which are GARCH(1, 1) processes.

$$\mathbf{r}_t = \mathbf{W}\mathbf{f}_t, \quad \mathbf{f}_t | \mathcal{F}_{t-1} \sim \mathcal{N}_N(\mathbf{0}, \mathbf{H}_t), \quad \mathbf{H}_t = \text{diag}(h_{1,t}, \dots, h_{N,t}),$$

$$\text{where } h_{i,t} = \omega_i + \alpha_{i,1} f_{i,t-1}^2 + \beta_{i,1} h_{i,t-1}, \quad t = 1, \dots, T; \quad i = 1, \dots, N,$$

with $w_{i,i'} \stackrel{\text{i.i.d.}}{\sim} \mathcal{N}(1, 1)$ for the loading matrix \mathbf{W} . For a randomly chosen $i \in \mathcal{S}_1 \subset \{1, \dots, N\}$, GARCH parameters of \mathbf{f} change at $\eta_1 = \lceil T/4 \rceil$ as in (M2.1)–(M2.2) (referred to as (M4.1)–(M4.2)). Another change-point is introduced to the loading matrix at $\eta_2 = \lceil 3T/5 \rceil$, by swapping the rows of \mathbf{W} corresponding to randomly chosen $i \in \mathcal{S}_2 \subset \{1, \dots, N\}$, which brings in a change in the conditional cross-correlations as well as within-series conditional variance. The cardinality of \mathcal{S}_1 and \mathcal{S}_2 is controlled as in (M2) with $\varrho \in \{1, 0.75, 0.5, 0.25\}$, and we consider $T = 500$ and $N \in \{50, 100\}$.

4.2 Results

Firstly, we performed the at-most-one-change test on the data simulated from (M0)–(M1) over 100 realisations by conducting only the first iteration of Algorithm 1, which enables us to investigate its size and power behaviour, respectively, along with the accuracy in change-point estimation; see Tables 1–3; results from (M1) when $N = 50$ can be found in the supplementary document.

Overall, we observe that our proposed methodology handles the high dimensionality of the data well both in terms of its size and power behaviour. When the innovations are generated from a Gaussian distribution with cross-correlations, the test manages to keep the size below the significance level $\alpha = 0.05$ when $N = 50$, while spurious false alarm is observed as the dimensionality grows for (M0.2). We note that, although not directly comparable, Table 1 of Fryzlewicz and Subba Rao (2014) observed similar size behaviour from their procedure as well as the change-point test from Andreou and Ghysels (2002) applied to univariate GARCH processes generated with the same GARCH parameters as in (M0.2). When the innovations are drawn from a t_{10} -distribution, the parameter configuration of (M0.2) brings in greater size distortion.

As expected, the test achieves higher power when the change-point is ‘dense’ cross-sectionally (with larger ρ) and located centrally, and the same applies to the location accuracy of the change-point estimator. For most GARCH parameter configurations, the test attains power above 0.9 even when the change-point is relatively sparse ($\rho = 0.25$), but for (M1.2), (M1.4) and (M1.8). Even when the location of the change-point is skewed ($\eta_1 = [0.9T]$), our method generally attains high power and location accuracy if the change-point is not too sparse, in most settings where it shows good performance when the change-point is centrally located ($\eta_1 = [T/2]$).

Tables 4 reports the results from applying the proposed methodology to multiple change-point detection from tv-MGARCH processes generated as described in (M2); the supplementary document contains figures summarising the locations of estimated change-points. When the change is restricted to GARCH parameters, it appears that the change-point that results

in time-varying $\text{var}(r_{i,t})$, $i \in \mathcal{S}_1$ (see (M2.1)–(M2.2), with (M2.1) bringing a change in a larger jump in the variance) are better detected than the change-point at which $\text{var}(r_{i,t})$, $i \in \mathcal{S}_1$ is kept approximately constant (see (M2.3)). Between the two types of change-points considered in (M2), the detection of η_1 is more challenging as it becomes sparser and N increases. It is explained by the fact that, the sparsity of η_1 , measured by the number of series containing η_1 scaled by d , is in the order of ϱN^{-1} whereas that of η_2 is in the order of ϱ^2 .

Tables 5–6 indicate that mis-specifying the GARCH orders (p, q) does not noticeably worsen the performance of our methodology, confirming the robustness of our methodology to the choice of p and q . For the full-factor MGARCH model in (M4), Table 7 shows that our methodology manages to estimate the two change-points with high accuracy, when their presence is detected, albeit the presence of spurious change-points (see also Figures 7–8 in the supplementary document). It shows that possible limitation of the re-sampling based choice of the threshold when the cross-sectional correlations are strong due to the presence of common factors.

Table 1: (M0) Size of the change-point test at $\alpha = 0.05$ when $T = 1000$.

n	Gaussian $\varepsilon_{i,t}$		t_{10} -distributed $\varepsilon_{i,t}$	
	(M0.1)	(M0.2)	(M0.1)	(M0.2)
50	0.01	0.05	0.03	0.13
100	0.02	0.09	0.02	0.3

Table 2: (M1) Power of the change-point test at $\alpha = 0.05$ and the accuracy of $\hat{\eta}_1$ when $N = 100$, $T = 1000$ and $\eta_1 = [T/2]$.

ϱ	(M1.1)		(M1.2)		(M1.3)		(M1.4)	
	power	accuracy (%)						
1	1.00	100	1.00	100	1.00	100	1.00	96
0.75	1.00	100	1.00	100	1.00	100	1.00	93
0.5	1.00	100	1.00	100	1.00	100	0.94	83
0.25	1.00	98	1.00	90	1.00	100	0.46	36
ϱ	(M1.5)		(M1.6)		(M1.7)		(M1.8)	
	power	accuracy (%)						
1	1.00	100	1.00	100	1.00	100	1.00	100
0.75	1.00	100	1.00	100	1.00	100	1.00	100
0.5	1.00	100	1.00	100	1.00	100	1.00	99
0.25	1.00	100	1.00	100	1.00	100	0.98	93

Table 3: (M1) Power of the change-point test at $\alpha = 0.05$ and the accuracy of $\hat{\eta}_1$ when $N = 100$, $T = 1000$ and $\eta_1 = [0.9T]$.

ϱ	(M1.1)		(M1.2)		(M1.3)		(M1.4)	
	power	accuracy (%)						
1	1.00	100	1.00	100	1.00	100	0.87	78
0.75	1.00	100	1.00	100	1.00	100	0.65	57
0.5	1.00	100	1.00	100	1.00	100	0.18	15
0.25	1.00	100	0.81	76	1.00	100	0.07	1

ϱ	(M1.5)		(M1.6)		(M1.7)		(M1.8)	
	power	accuracy (%)						
1	1.00	100	1.00	100	1.00	100	1.00	98
0.75	1.00	100	1.00	100	1.00	100	1.00	97
0.5	1.00	100	1.00	100	1.00	100	0.93	84
0.25	1.00	100	0.52	52	1.00	100	0.31	26

Table 4: (M2) The number of estimated change-points (%) and the accuracy in change-point location when $\alpha = 0.05$, $N = 50$ (left), $N = 100$ (right) and $T = 500$.

ϱ	\hat{B}					accuracy (%)		\hat{B}					accuracy (%)		
	0	1	2	3	≥ 4	η_1	η_2	0	1	2	3	≥ 4	η_1	η_2	
	(M2.1)	1	0	0	100	0	0	100	100	0	0	100	0	0	100
	0.75	0	0	100	0	0	100	100	0	0	100	0	0	100	100
	0.5	0	0	100	0	0	100	100	0	0	100	0	0	100	100
	0.25	0	7	92	1	0	100	93	0	91	9	0	0	100	6
(M2.2)	1	0	0	100	0	0	100	100	0	0	100	0	0	100	100
	0.75	0	2	98	0	0	96	100	0	0	100	0	0	100	100
	0.5	0	38	62	0	0	60	100	0	2	98	0	0	98	100
	0.25	0	95	5	0	0	2	100	0	80	20	0	0	32	84
(M2.3)	1	0	89	11	0	0	3	100	0	68	31	1	0	13	100
	0.75	0	89	11	0	0	3	100	0	85	15	0	0	3	100
	0.5	0	94	6	0	0	0	100	0	88	12	0	0	3	100
	0.25	0	97	3	0	0	0	100	1	96	3	0	0	0	98

Table 5: (M3.1) The number of estimated change-points (%) and the accuracy in change-point location when $\alpha = 0.05$, $N = 50$ (left), $N = 100$ (right) and $T = 500$.

ϱ	\hat{B}					accuracy (%)		\hat{B}					accuracy (%)		
	0	1	2	3	≥ 4	η_1	η_2	0	1	2	3	≥ 4	η_1	η_2	
(M3.1.1)	1	0	0	98	2	0	100	100	0	0	100	0	0	100	100
	0.75	0	0	100	0	0	100	100	0	0	99	1	0	100	100
	0.5	0	0	95	5	0	100	100	0	0	100	0	0	100	100
	0.25	0	18	73	8	1	100	80	0	97	3	0	0	100	1
(M3.1.2)	1	0	1	97	2	0	99	100	0	0	99	1	0	100	100
	0.75	0	8	90	2	0	92	100	0	0	99	1	0	100	100
	0.5	0	50	47	3	0	46	100	0	7	85	8	0	93	100
	0.25	1	88	10	1	0	5	99	3	79	18	0	0	27	78

Table 6: (M3.2) The number of estimated change-points (%) and the accuracy in change-point location when $\alpha = 0.05$, $N = 50$ (left), $N = 100$ (right) and $T = 500$.

	ϱ	\hat{B}					accuracy (%)		\hat{B}					accuracy (%)	
		0	1	2	3	≥ 4	η_1	η_2	0	1	2	3	≥ 4	η_1	η_2
(M3.2.1)	1	0	0	100	0	0	100	100	0	0	100	0	0	100	100
	0.75	0	0	98	2	0	100	100	0	0	98	2	0	100	100
	0.5	0	0	99	1	0	100	100	0	0	99	1	0	100	100
	0.25	0	5	92	2	1	95	100	0	15	74	11	0	100	83
(M3.2.2)	1	0	0	99	1	0	100	100	0	0	100	0	0	100	100
	0.75	0	0	97	3	0	100	100	0	0	99	1	0	100	100
	0.5	0	0	98	2	0	100	100	0	0	98	2	0	100	100
	0.25	0	45	51	4	0	48	100	0	12	79	9	0	92	93

Table 7: (M4) The number of estimated change-points and the accuracy in change-point location when $\alpha = 0.05$, $N = 50$ (left), $N = 100$ (right) and $T = 500$.

	ϱ	\hat{B}					accuracy (%)		\hat{B}					accuracy (%)	
		0	1	2	3	≥ 4	η_1	η_2	0	1	2	3	≥ 4	η_1	η_2
(M4.1)	1	0	5	34	52	9	91	97	0	0	45	44	11	95	97
	0.75	0	3	36	49	12	95	90	0	0	33	60	7	95	96
	0.5	0	4	37	52	7	89	89	0	3	17	64	16	96	88
	0.25	0	14	42	39	5	77	53	0	6	32	48	14	92	70
(M4.2)	1	0	13	87	0	0	87	99	0	4	96	0	0	96	98
	0.75	0	22	78	0	0	79	96	0	7	93	0	0	93	97
	0.5	0	74	24	2	0	29	93	0	38	61	1	0	64	97
	0.25	6	89	5	0	0	8	70	0	93	7	0	0	8	92

5 Real data analysis

In this section, we examine the effect of ignoring possible changes in the volatility and correlation of a multi-asset portfolio, and apply our method to calculate the Value-at-Risk (VaR) of a portfolio, a widely used measure of market risk embraced by financial institutions for regulatory or other internal purposes.

5.1 VaR, stressed VaR and its backtests

VaR measures the extreme loss (change in value) of an asset or a portfolio of assets with a prescribed probability level during a given holding period. It has been criticised due to its unrealistic assumptions (linearity and normality), parameter sensitivity (to estimation and holding periods) and its inadequacy during crises especially when correlations between assets are observed to vary over time (Persaud, 2000; Danielsson, 2002). The last point is of particular interest, since compared to the period of market stability, correlations are observed to be significantly higher when markets are falling (Li et al., 2017). Jäckel and Rebonato (2001) noted that a risk manager ‘would greatly over-estimate the degree of diversification in his portfolio in the event of a crash if he used the [correlation] matrix estimated during normal periods’. Works to address the criticism on VaR exist: Valentinyi-Endrész (2004) examined whether detecting and taking into account change-points improves upon VaR forecast. Similarly, Spokoiny (2009) proposed the local change-point analysis to detect regions of volatility homogeneity as an alternative to stationary GARCH modelling, and found that the local volatility estimator performed well in the application to VaR.

The Basel Accord (1996 Amendment) requires the use of stressed VaR (sVaR) which is based on a covariance matrix from a crisis period in the past. The accord does not specify the exact time period to be used but instead proposes the *judgement-based* and the *formulaic* approaches (European Banking Authority, 2012). The former relies on a high-level analysis of the risks related to the holding portfolio, while the latter is a more systematic, quantitative approach where our proposed methodology can contribute to providing a robust risk management, by supplying the information about the latest stressed periods.

We first introduce the VaR metric which can be formulated as follows:

$$\text{VaR}_t(\alpha) = -F^{-1}(\alpha|\mathcal{G}_t),$$

where $F^{-1}(\cdot|\mathcal{G}_t)$ is the quantile function of the loss and profit distribution. This distribution changes over time due to market and portfolio specific conditions, which is embodied in \mathcal{G}_t . The accuracy of a model to estimate VaR is tested by examining the null hypothesis that the observed probability of occurrence over a specified horizon is equal to the probability level α , the violation of which signals concerns. Typically, a financial institution should backtest its VaR by means of statistical tests before reporting it to the interested parties, e.g., stakeholders and regulators. [Kupiec \(1995\)](#) proposes two methods, the Proportion of Failure (PoF) and the Time until First Failure (TFF), to accomplish this. For a sample of T observations, the Kupiec test statistics takes the form of likelihood ratio

$$LR_{PoF} = -2 \log \left(\frac{(1 - \alpha)^{T-x_f} \alpha^{x_f}}{\left(1 - \frac{x_f}{T}\right)^{T-x_f} \left(\frac{x_f}{T}\right)^{x_f}} \right) \quad \text{and} \quad LR_{TFF} = -2 \log \left(\frac{\alpha(1 - \alpha)^{t_f-1}}{\left(\frac{1}{t_f}\right) \left(1 - \frac{1}{t_f}\right)^{t_f-1}} \right),$$

where x_f denotes the number of failures occurred and t_f the number of days until the first failure within the T observations. Under H_0 , both LR_{PoF} and LR_{TFF} are asymptotically χ_1^2 -distributed, and their exceedance of the critical value implies that the VaR model is inadequate.

However, these tests cannot control for the dependence of violations, i.e., violations may cluster while the overall (unconditional) average of violations is not significantly different from αT . To address this limitation, a regression-based test is proposed by [Engle and Manganelli \(2004\)](#). Formally, let us define $Hit_t(\alpha) = \mathbb{I}(r_t < -\text{VaR}_t(\alpha)) - \alpha$ where r_t is the time series of portfolio returns. The function $Hit_t(\alpha)$ assumes the value $1 - \alpha$ when r_t is less than the VaR level α and $-\alpha$ otherwise. The unconditional expectation of $Hit_t(\alpha)$ is, obviously, zero. The conditional expectation should also be zero meaning that $Hit_t(\alpha)$ is uncorrelated with its own past and other lagged variables (such as r_t , r_t^2 or the one-step ahead forecast VaR). To test this assumption, the dynamic conditional quantile (DQ) test is adopted which involves

the following statistic

$$DQ = T^{-1}(\mathbf{Hit}^\top \mathbf{X}(\mathbf{X}^\top \mathbf{X})^{-1} \mathbf{X}^\top \mathbf{Hit})/\alpha(1 - \alpha)$$

where \mathbf{X} is the matrix of explanatory variables (e.g., raw and squared past returns) and \mathbf{Hit} the vector collecting $Hit_t(\alpha)$. Under the null hypothesis, [Engle and Manganelli \(2004\)](#) show that the proposed statistic DQ follows a $\chi_{\bar{q}}^2$ where $\bar{q} = \text{rank}(\mathbf{X})$.

We use these three backtests to examine the performance of our method in the applications to stressed VaR.

5.2 Detecting change-points in a multi-asset portfolio

We collect the daily US Treasury zero-coupon yield curves from the US Federal Reserve Board, which are based on a large set of outstanding bonds and notes with maturity from 1 to 30 years, as well as the daily prices of S&P500 index, see [Figure 1](#). The unconditional correlations between the 30 log-differenced Treasury price time series range from 0.787 to 0.994. The thirty time series along with the log-returns of the S&P500 index, from 1 January 2000 to 31 December 2014 (the training set), serve as an input to our methodology for change-point detection ($N = 31$, $d_N = 496$ and $T = 3730$). For validation of our method, we also collect the same data from 1 January 2015 to 31 December 2016 which serves as the out-of-sample test set. We form a portfolio by allocating 50% on S&P500 and the remaining 50% equally on the 30 Treasury bonds to avoid creating a portfolio consisting mainly of bonds. We also de-mean the return vector, albeit this does not change the results.

Our method, using the default parameters described in [Section 3.3](#) and the re-sampling scheme described in [Section 3.4](#), returns three change-points and therefore four periods as reported in [Table 8](#) (Periods 1–4). The same table also reports Period 5, which covers the 12-month period following the bankruptcy of Lehman Brothers in September 2008 as the crisis period, with its length chosen in accordance with Basel 2.5 ([Basle Committee on Banking Supervision, 2010](#)). The results indicate that the highest VaR (found by simply calculating the quantiles of the portfolio returns and taking the modulus) was obtained from the period

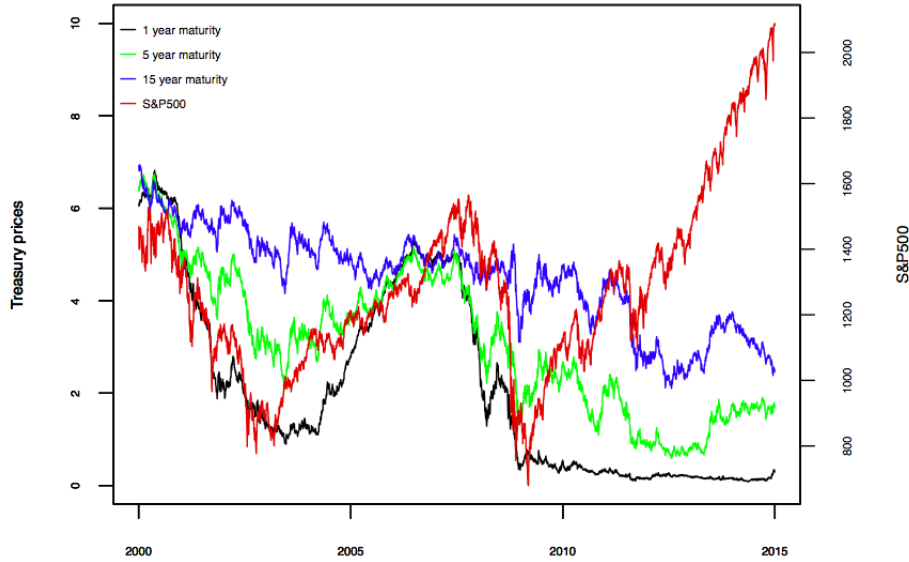


Figure 1: Daily Treasury prices for three different maturities (left y -axis) and the S&P500 index (right y -axis).

spanning from 11 September 2008 to 26 March 2009 (Period 3), a rather expected outcome given the high volatility that the markets experienced after the Lehman Brothers bankruptcy. We note that this period spans less than 12 months, and is shorter than the maximum allowed duration by Basel 2.5. It also coincides with the Bank of England’s view on the historical periods per region with the worst market moves ([Bank of England \(2018\)](#)). Period 4 also exhibits high stress characteristics, but less severe than those from the aftermath of the Lehman Brothers collapse. If a bank selects Period 5 (the 99% VaR of which is 4.95%) to calibrate its sVaR model, it will likely under-estimate the measure compared to that calibrated with Period 3 for which the 99% VaR is 5.39%. In the remainder of this section, we explore this argument in detail.

In order to assess which stressed period is the most appropriate for an sVaR measure, we conduct two exercises: the historical simulation (unconditional, [Section 5.3](#)) and the conditional covariance modelling using the DCC model of [Engle \(2002\)](#) ([Section 5.4](#)). The former is the most popular VaR model used by banks, and the latter is a natural choice given the underlying time-varying multivariate model of our proposed method. We note that our proposed methodology serves as a change-point detection technique, and does not automatically lead to the choice of a VaR (sVaR) model. Our suggestion is, after the change-points are

estimated from a given dataset, a user should decide on the VaR model separately based on regulatory or internal requirements.

Table 8: The table reports the three change-points detected by our methodology (bold) from 1 January 2000 to 31 December 2014, and the corresponding periods of stationarity. In addition, for each period it also reports the 95% and 99% VaR of a portfolio with 50% allocated on S&P500 and the rest 50% equally on the 30 Treasury bonds.

	Period range		Value-at-Risk	
	From	Until	95%	99%
Period 1	01/01/2000	31/12/2007	0.01267	0.01793
Period 2	01/02/2008	11/09/2008	0.01834	0.02597
Period 3	12/09/2008	26/03/2009	0.03809	0.05392
Period 4	27/03/2009	31/12/2014	0.01912	0.02708
Period 5	12/09/2008	14/09/2009	0.03496	0.04951

5.3 sVaR calculation using historical simulation

We consider the vector of the returns \mathbf{r}_t , its covariance matrix $\Sigma_r(t)$ and portfolio weights \mathbf{w} (allocating 50% to S&P and the rest to the Treasury bonds equally divided) for the test period. We index the five periods identified in Table 8 with $b = 1, \dots, 5$ and denote the unconditional covariance matrix for each regime by $\Sigma_r^{(b)}$. A financial institution typically uses historical simulation over one year (roughly $T_{sv} = 250$ days) to forecast the 1-day ahead sVaR, as

$$\widehat{\text{sVaR}}_{t+1}^b = -\left[\text{upper } 100 \times \alpha\text{-th percentile of } \{R_\tau^b\}_{\tau=t-T_{sv}+1}^t \right], \quad (11)$$

$$\text{where } R_t^b = \mathbf{r}_t^\top \{\mathbf{L}^{(b)}\mathbf{L}(t)\}^{-1} \mathbf{w} \quad (12)$$

with $\mathbf{L}^{(b)}$ being the Cholesky decomposition of $\Sigma_r^{(b)}$ and $\mathbf{L}(t)$ the Cholesky decomposition of $\Sigma_r(t)$. Equation (12) transforms the return vector \mathbf{r}_t with covariance matrix $\Sigma_r(t)$ into the portfolio return R_t^b of a return vector with a (stressed) covariance $\Sigma_r^{(b)}$, for each $b = 1, \dots, 5$ (see Duffie and Pan (1997)). To estimate $\Sigma_r(t)$, we use the data from 1 January 2015 to 31 December 2015. For each b , we repeatedly forecast the 1-day ahead sVaR using $\widehat{\text{sVaR}}_{t+1}^b$ in (11) by rolling the 250-day estimation window forward one day at a time until we reach the end of the time series on 31 December 2016.

The results from sVaR backtesting using the historical simulation approach are provided in Table 9 for $\alpha = 0.01$ and 0.05 , and Figure 2 displays $\widehat{\text{sVaR}}_{t+1}^b$ obtained with $\alpha = 0.01$ along with the daily portfolio return. In particular, the table indicates that Period 3 can be safely used to calibrate sVaR. The number of failures is far below the expected number of violations for the 250 day period at 95% and 99% levels (12 and 2, respectively). Note that the alternative hypothesis in the PoF test is two-side and a small number of violations will also reject the adequacy of an sVaR model. The sVaR model calibrated using Period 3 yields a favourable, albeit conservative, result and is more likely to be accepted by the regulators. Besides, it passes the traffic light test ([Basle Committee on Banking Supervision, 1996](#)), whereby a VaR model is deemed valid if the cumulative probability of observing up to x_f failures is less than 0.95 (green zone) under the binomial distribution with T_{sv} and α as the parameters. Testing the same period using the TFF test, the first failure occurred only after 120 days at the 95% level and there was no violation at the 99% level (the TFF test is also two-side). The results of the DQ tests confirm that Period 3 is the best candidate for the sVaR calibration. Period 5 also exhibited a small number of violations, rather expected behaviour considering that it overlaps with Period 3 for nine months.

Table 9: sVaR backtesting using the historical simulation approach calibrated on five different stress periods. The table reports the number of sVaR violations (PoF, top); the number of days until the first violation in sVaR (TFF, middle); the DQ test statistic (bottom). Small p -values (given in brackets) indicate the rejection of H_0 : the sVaR measure is adequate.

	Period 1	Period 2	Period 3	Period 4	Period 5
	PoF				
99%	8 (0.00)	2 (0.75)	0 (0.02)	4 (0.37)	1 (0.28)
95%	19 (0.07)	7 (0.08)	1 (0.00)	11 (0.67)	1 (0.00)
	TFF				
99%	9 (0.07)	120 (0.85)	-	20 (0.19)	120 (0.85)
95%	2 (0.06)	7 (0.35)	120 (0.01)	7 (0.86)	120 (0.01)
	DQ				
99%	70.16 (0.00)	85.56 (0.00)	2.45 (0.96)	86.08 (0.00)	1.70 (0.98)
95%	22.56 (0.00)	16.43 (0.03)	10.90 (0.20)	9.91 (0.27)	10.88 (0.20)

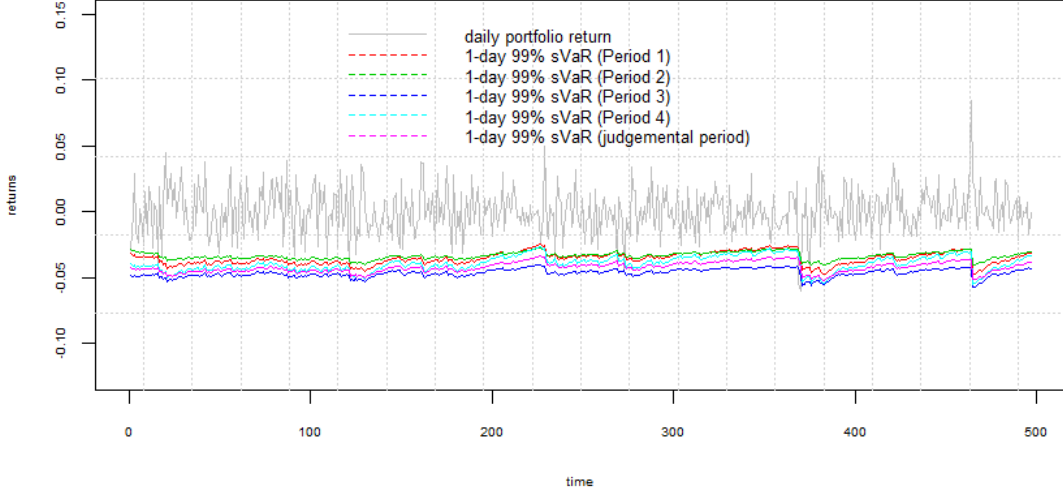


Figure 2: Returns of a portfolio of US Treasury zero-coupon bonds (50%) and the S&P500 index (50%) for the testing (rolling) period. The coloured lines indicate the one-day ahead forecast of sVaR in (11) obtained from the historical simulation using the five periods in Table 8 as the stressed period.

5.4 sVaR calculation using a conditional covariance model

In the second exercise, we adopt the DCC model of Engle (2002) in which the conditional covariance is factorised as

$$\mathbf{H}_t = \mathbf{D}_t \mathbf{R}_t \mathbf{D}_t \quad (13)$$

where $\mathbf{D}_t = \text{diag}(h_{1,t}^{1/2}, \dots, h_{N,t}^{1/2})$ and $h_{i,t}$, $i = 1, \dots, N$ follows the conditional variance GARCH(p, q) model

$$h_{i,t} = \omega_i + \sum_{j=1}^p \alpha_{i,j} r_{i,t-j}^2 + \sum_{k=1}^q \beta_{i,k} h_{i,t-k}. \quad (14)$$

The model (14) is the stationary version of the model (1) as we estimate the DCC within each stationary segment identified by our change-point detection methodology. Engle (2002) proposes the following dynamic correlation structure

$$\boldsymbol{\Sigma}_t = (1 - a_{dcc} - b_{dcc}) \bar{\boldsymbol{\Sigma}} + a_{dcc} \mathbf{v}_{t-1} \mathbf{v}_{t-1}^\top + b_{dcc} \boldsymbol{\Sigma}_{t-1} \quad (15)$$

$$\mathbf{R}_t = \text{diag}(\boldsymbol{\Sigma}_t)^{-1/2} \boldsymbol{\Sigma}_t \text{diag}(\boldsymbol{\Sigma}_t)^{-1/2} \quad (16)$$

where $\mathbf{v}_t = \mathbf{D}_t^{-1} \mathbf{r}_t$ is the standardised residual vector, and $\bar{\boldsymbol{\Sigma}} = [\rho_{i,j}]_{i,j=1}^N$ with $\rho_{i,j}$ denoting

the unconditional sample correlations between $v_{i,t}$ and $v_{j,t}$.

Similarly to the approach taken in Section 5.3, we consider a portfolio of assets with the return vector \mathbf{r}_t , its covariance matrix $\Sigma_r(t)$ and the vector of portfolio weights \mathbf{w} over the test period. Here, we set \mathbf{w} so that it allocates 50% on the S&P500 index and the remaining 50% equally on the ten Treasury bonds with the highest maturity. This is because the estimation of DCC becomes numerically unstable with all thirty Treasury bonds included. For the b -th stationary segment, we estimate a DCC model and obtain the parameters $\hat{a}_{dcc}, \hat{b}_{dcc}$ along with $\hat{\omega}_i, \hat{\alpha}_{i,j}, \hat{\beta}_{i,j}$ of the individual GARCH models. We consider GARCH(1,1) with normally distributed innovations for maximum likelihood estimation, but results were similar with other model orders p, q or innovations. With the estimated DCC parameters for each segment, we obtain the 1-day ahead forecast of the covariance matrix, $\hat{\Sigma}_{t+1}^{(b)}$, applying (15) to the data from 1 January 2015. Finally, we forecast the portfolio volatility

$$\hat{\sigma}_{t+1}^{(b)} = \sqrt{\mathbf{w}^\top \hat{\Sigma}_{t+1}^{(b)} \mathbf{w}} \quad \text{for } b = 1, \dots, 5,$$

and compare $-1.96 \times \hat{\sigma}_{t+1}^{(b)}$ (95% sVaR up to its sign) and $-2.33 \times \hat{\sigma}_{t+1}^{(b)}$ (99% sVaR) to the actual portfolio returns.

The backtesting results are given in Table 10. Using the estimated parameters from Period 3 resulted in the smallest number of violations compared with the rest. At the 99% level, the first violation occurred after 121 days compared to the 16 days taken for Periods 1,2,4 and 5. The DQ test also indicates that Period 3 is the most suitable for calibrating the 95% sVaR metric. This is not the case for the 99% case, but there were not enough observations (three violations) for a reliable calculation of the DQ statistic.

6 Conclusions

In this paper, we propose a methodology for detecting multiple change-points in both within-series and cross-correlation structures of multivariate volatility processes. The two-stage methodology first transforms the N -dimensional series so that the structural change-points

Table 10: sVaR backtesting using the DCC model calibrated on five different stress periods. The table reports the number of sVaR violations (PoF, top); the number of days until the first violation in sVaR (TFF, middle); the DQ test statistic (bottom). Small p -values (given in brackets) indicate the rejection of H_0 : the sVaR measure is adequate.

	Period 1	Period 2	Period 3	Period 4	Period 5
	PoF				
99%	7 (0.38)	7 (0.38)	3 (0.33)	7 (0.38)	7 (0.38)
95%	36 (0.01)	20 (0.30)	13(0.00)	27 (0.66)	24 (0.86)
	TFF				
99%	16 (0.15)	16 (0.15)	121 (0.84)	16 (0.15)	16 (0.15)
95%	1 (0.01)	1 (0.01)	16 (0.82)	16 (0.82)	1 (0.01)
	DQ				
99%	33.01 (0.00)	31.72 (0.00)	39.78 (0.00)	31.50 (0.00)	31.46 (0.00)
95%	15.85 (0.02)	13.23 (0.06)	10.10 (0.18)	7.53 (0.37)	15.20 (0.03)

are detectable as change-points in the means of $N(N + 1)/2$ -dimensional transformed data, which serves as an input to the multiple change-point detection algorithm in the second stage. We show the consistency of the methodology in terms of the total number and locations of estimated change-points, and propose a bootstrap procedure for threshold selection, which shows reasonably good performance in our simulation studies. Finally, we apply the proposed method to demonstrate its usage in identifying periods of ‘stress’ in a multivariate financial dataset consisting of thirty US Treasury zero-coupon yield curves and the S&P500 index. This exercise indicates the efficacy of our methodology in risk management tasks, such as when calculating the (stressed) Value-at-Risk of a portfolio of risky assets.

Acknowledgements

Haeran Cho’s work was supported by the Engineering and Physical Sciences Research Council grant no. EP/N024435/1.

References

Andreou, E. and E. Ghysels (2002). Detecting multiple breaks in financial market volatility dynamics. *Journal of Applied Econometrics* 17(5), 579–600.

- Andreou, E. and E. Ghysels (2003). Tests for breaks in the conditional co-movements of asset returns. *Statistica Sinica* 13, 1045–1073.
- Baele, L. (2003). Did emu increase equity market correlations? *Financieel Forum, Bank en Financiewezen* 6, 356–359.
- Baillie, R. T. and Bollerslev, T. (1991). Intra-day and inter-market volatility in foreign exchange rates. *The Review of Economic Studies* 58(3), 565–585.
- Bank of England (2018). *Stress testing the UK banking system: guidance on the traded risk methodology for participating banks and building societies*. <https://www.bankofengland.co.uk/-/media/boe/files/stress-testing/2018/stress-testing-the-uk-banking-system-2018-guidance.pdf>.
- Barassi, M., L. Horváth, and Y. Zhao (2018). Change point detection in the conditional correlation structure of multivariate volatility models. *Journal of Business & Economic Statistics* (to appear).
- Barigozzi, M., H. Cho, and P. Fryzlewicz (2018). Simultaneous multiple change-point and factor analysis for high-dimensional time series. *Journal of Econometrics* 206(1), 187–225.
- Basle Committee on Banking Supervision (1996). *Supervisory Framework for the Use of ‘Backtesting’ in Conjunction with the Internal Models Approach to Market Risk Capital Requirements*. <https://www.bis.org/publ/bcbsc223.pdf>.
- Basle Committee on Banking Supervision (2010). *Revisions to the Basel II market risk framework*. <https://www.bis.org/publ/bcbs193.pdf>.
- Bauwens, L., S. Laurent, and J. V. Rombouts (2006). Multivariate garch models: a survey. *Journal of Applied Econometrics* 21(1), 79–109.
- Berkes, I., L. Horváth, and P. Kokoszka (2004). Testing for parameter constancy in garch(p, q) models. *Statistics and Probability Letters* 70(4), 263–273.

- Bollerslev, T. (1990). Modelling the coherence in short-run nominal exchange rates: a multivariate generalized arch model. *The Review of Economics and Statistics*, 498–505.
- Bollerslev, T., R. F. Engle, and J. M. Wooldridge (1988). A capital asset pricing model with time-varying covariances. *Journal of Political Economy* 96(1), 116–131.
- Boussama, F., F. Fuchs, and R. Stelzer (2011). Stationarity and geometric ergodicity of bekk multivariate garch models. *Stochastic Processes and their Applications* 121, 2331–2360.
- Cappiello, L., R. F. Engle, and K. Sheppard (2006). Asymmetric dynamics in the correlations of global equity and bond returns. *Journal of Financial Econometrics* 4(4), 537–572.
- Cho, H. (2016). Change-point detection in panel data via double cusum statistic. *Electronic Journal of Statistics* 10(2), 2000–2038.
- Cho, H. and P. Fryzlewicz (2015). Multiple change-point detection for high-dimensional time series via sparsified binary segmentation. *Journal of the Royal Statistical Society: Series B* 77(2), 475–507.
- Csörgö, M. and L. Horváth (1997). *Limit Theorems in Change-point Analysis*, Volume 18. John Wiley & Sons Inc.
- Danielsson, J. (2002). The emperor has no clothes: Limits to risk modelling. *Journal of Banking & Finance* 26(7), 1273–1296.
- De Pooter, M. and D. Van Dijk (2004). Testing for changes in volatility in heteroskedastic time series – a further examination. Technical report, Econometric Institute.
- Dette, H., G. M. Pan, and Q. Yang (2018). Estimating a change point in a sequence of very high-dimensional covariance matrices. *arXiv preprint, arXiv:1807.10797*.
- Diebold, F. and A. Inoue (2001). Long range and regime switching. *Journal of Econometrics* 105(1), 131–159.
- Douc, R., E. Moulines, and D. Stoffer (2014). *Nonlinear Time Series: Theory, Methods and Applications with R Examples*. Chapman and Hall/CRC.

- Du, X., L. Y. Cindy, and D. J. Hayes (2011). Speculation and volatility spillover in the crude oil and agricultural commodity markets: A bayesian analysis. *Energy Economics* 33(3), 497–503.
- Duffie, D. and J. Pan (1997). An overview of value at risk. *The Journal of Derivatives* 4(3), 7–49.
- Engle, R. (2002). Dynamic conditional correlation: A simple class of multivariate generalized autoregressive conditional heteroskedasticity models. *Journal of Business & Economic Statistics* 20(3), 339–350.
- Engle, R. F. and K. F. Kroner (1995). Multivariate simultaneous generalized arch. *Econometric Theory* 11(01), 122–150.
- Engle, R. F. and S. Manganelli (2004). CAViaR: Conditional autoregressive value at risk by regression quantiles. *Journal of Business & Economic Statistics* 22(4), 367–381.
- European Banking Authority (2012). *Guidelines on Stressed Value At Risk*. <https://www.eba.europa.eu/documents/10180/104547/EBA-BS-2012-78--GL-on-Stressed-VaR-.pdf>.
- Ewing, B. T. and F. Malik (2013). Volatility transmission between gold and oil futures under structural breaks. *International Review of Economics & Finance* 25, 113–121.
- Fan, J., M. Wang, and Q. Yao (2008). Modelling multivariate volatilities via conditionally uncorrelated components. *Journal of the Royal Statistical Society: Series B* 70(4), 679–702.
- Fryzlewicz, P. and S. Subba Rao (2011). Mixing properties of arch and time-varying arch processes. *Bernoulli* 17(1), 320–346.
- Fryzlewicz, P. and S. Subba Rao (2014). Multiple-change-point detection for auto-regressive conditional heteroscedastic processes. *Journal of the Royal Statistical Society: Series B*, 903–924.
- Hamilton, J. D. (2003). What is an oil shock? *Journal of Econometrics* 113(2), 363–398.

- Hansen, C. S. (2001). The relation between implied and realised volatility in the danish option and equity markets. *Accounting & Finance* 41(3), 197–228.
- Hansen, P. R. and A. Lunde (2005). A forecast comparison of volatility models: does anything beat a garch(1, 1)? *Journal of Applied Econometrics* 20(7), 873–889.
- Horváth, L. and M. Hušková (2012). Change-point detection in panel data. *Journal of Time Series Analysis* 33(4), 631–648.
- Jäckel, P. and R. Rebonato (2001). Valuing american options in the presence of user defined smiles and time-dependent volatility: Scenario analysis, model stress and lower bound pricing applications. *Journal of Risk* 4(1), 35–61.
- Jirak, M. (2015). Uniform change point tests in high dimension. *The Annals of Statistics* 43(6), 2451–2483.
- Kokoszka, P. and R. Leipus (2000). Change-point estimation in arch models. *Bernoulli* 6(3), 513–539.
- Kokoszka, P. and G. Teyssière (2002). Change-point detection in garch models: asymptotic and bootstrap tests. Technical report, Universite Catholique de Louvain.
- Korostelev, A. (1987). On minimax estimation of a discontinuous signal. *Theory of Probability & its Applications* 32(4), 727–730.
- Kupiec, P. H. (1995). Techniques for verifying the accuracy of risk measurement models. *The Journal of Derivatives* 3(2), 73–84.
- Lee, S., Y. Tokutsu, and K. Maekawa (2003). The residual cusum test for the constancy of parameters in garch(1, 1) models. Technical report, Seoul National University.
- Li, J., V. Todorov, G. Tauchen, and H. Lin (2017). Rank tests at jump events. *Journal of Business & Economic Statistics*, 1–10.
- Mikosch, T. and C. Stărică (2004). Nonstationarities in financial time series, the long-range dependence, and the igarch effects. *The Review of Economics and Statistics* 86(1), 378–390.

- Persaud, A. (2000). Sending the herd off the cliff edge: the disturbing interaction between herding and market-sensitive risk management practices. *The Journal of Risk Finance* 2(1), 59–65.
- Pesaran, M. H. and A. Timmermann (2007). Selection of estimation window in the presence of breaks. *Journal of Econometrics* 137(1), 134–161.
- Ross, S. A. (1989). Information and volatility: The no-arbitrage martingale approach to timing and resolution irrelevancy. *The Journal of Finance* 44(1), 1–17.
- Spokoiny, V. (2009). Multiscale local change point detection with applications to value-at-risk. *The Annals of Statistics* 37, 1405–1436.
- Stock, J. H. and M. W. Watson (2002). Macroeconomic forecasting using diffusion indexes. *Journal of Business & Economic Statistics* 20(2), 147–162.
- Valentinyi-Endr sz, M. (2004). Structural breaks and financial risk management. Technical report, Magyar Nemzeti Bank (Central Bank of Hungary).
- Van der Weide, R. (2002). Go-garch: a multivariate generalized orthogonal garch model. *Journal of Applied Econometrics* 17(5), 549–564.
- Venkatraman, E. S. (1992). Consistency results in multiple change-point problems. *Technical Report No. 24, Department of Statistics, Stanford University*.
- Vostrikova, L. J. (1981). Detecting ‘disorder’ in multidimensional random processes. *Soviet Doklady Mathematics* 24, 55–59.
- Vrontos, I. D., P. Dellaportas, and D. N. Politis (2003). A full-factor multivariate garch model. *The Econometrics Journal* 6(2), 312–334.
- Wang, D., Y. Yu, and A. Rinaldo (2018). Optimal covariance change point detection in high dimension. *arXiv preprint arXiv:1712.09912*.
- Wang, T. and R. J. Samworth (2018). High dimensional change point estimation via sparse projection. *Journal of the Royal Statistical Society: Series B* 80, 57–83.